Available online at www.sciencedirect.com
ScienceDirect
Scripta Materialia 64 (2011) 725–728
Scripta MATERIALIA
www.elsevier.com/locate/scriptamat

Load-biased shape-memory and superelastic properties of a precipitation strengthened high-temperature $Ni_{50.3}Ti_{29.7}Hf_{20}$ alloy

G.S. Bigelow,[a,*] A. Garg,[a,b] S.A. Padula II,[a] D.J. Gaydosh[a,c] and R.D. Noebe[a]

[a]*Structures and Materials Division, 21000 Brookpark Rd., NASA Glenn Research Center, Cleveland, OH 44109, USA*
[b]*2801 W. Bancroft, University of Toledo, Toledo, OH 43606, USA*
[c]*22800 Cedar Point Road, Ohio Aerospace Institute, Cleveland, OH 44142, USA*

Received 9 November 2010; revised 17 December 2010; accepted 20 December 2010
Available online 24 December 2010

A slightly Ni-rich NiTi–20Hf (at.%) alloy was aged for 3 h at 550 °C to form a homogeneous distribution of 10–20 nm precipitates. To determine the effect of such structures on the martensite–austenite transformation, preliminary load-biased shape-memory and superelastic properties were measured. The alloy exhibited reasonably high transformation temperatures, near-perfect dimensional stability and a work output as high as 18.7 J cm^{-3} during load-biased thermal cycling. Isothermal stress cycling of the austenite between 180 and 220 °C resulted in near-perfect superelastic behavior up to 3% applied strain.
Published by Elsevier Ltd. on behalf of Acta Materialia Inc.

Keywords: Shape memory alloys; Martensitic phase transformation; Precipitation; Tension test; Transformation strain

NiTiHf has long been studied as a lower cost alternative to Au, Pd and Pt containing HTSMAs. In particular, the properties of (Ti + Hf)-rich NiTiHf alloys have been extensively studied because of the high transformation temperatures on that side of stoichiometry [1]. However, a wide hysteresis, low martensite finish (M_F) temperature, problems with fabrication, and poor dimensional and thermal stability have plagued these alloys and prevented any commercial application [2]. Recently, Meng et al. studied aging, precipitation [3], and one- and two-way shape memory behavior [4] of Ni-rich NiTiHf alloys which appear very promising.

In NiTi-based alloys, large second phases are present in both Ti-rich ($Ti_2Ni/Ti_4Ni_2O_x$-type) and far Ni-rich ($TiNi_3$-type) compositions [5]. However, if slightly Ni-rich compositions are chosen in NiTi and NiTiHf alloys, they can be heat treated to produce fine, nanoscale Ni-rich precipitates [6–8] that not only strengthen the matrix, but also result in a partial recovery of the transformation temperatures. In the NiTiHf system a peak martensite temperature (M_p) as high as ~230 °C has been reported in slightly Ni-rich 20 at.% Hf [9] compared to ~300 °C for Ti-rich (or stoichiometric) 20 at.% Hf alloys [10]. However, the load-biased shape memory and superelastic behavior of Ni-rich NiTiHf alloys have not been previously determined. Given these relatively high transformation temperatures and the fact that a high density of fine precipitates would strengthen a Ni-rich NiTiHf alloy matrix against slip and other deformation mechanisms, we have performed preliminary testing on an aged $Ni_{50.3}Ti_{29.7}Hf_{20}$ alloy to determine the shape memory and superelastic behavior of such a material.

A high-temperature shape memory alloy with a Ni-rich target composition of $Ni_{50.3}Ti_{29.7}Hf_{20}$ (at.%) was vacuum induction melted in a graphite crucible under a protective argon atmosphere using high-purity elemental materials (99.98% Ni, 99.95% Ti and 99.9% Hf). The resulting melt was cast into a 25.4 mm diameter by 102 mm long copper mold. After vacuum homogenization at 1050 °C for 72 h, the ingot was sealed in a mild steel can and extruded at 900 °C with an area reduction ratio of 7:1.

Mechanical test samples were machined from the extruded rod using a CNC lathe to form cylindrical dog-bone-shaped samples with a 5 mm diameter by 17.8 mm long gage section with threaded button ends. This geometry was designed to allow both tensile and compressive

* Corresponding author. Tel.: +1 216 433 6603; e-mail addresses: glen.s.bigelow@nasa.gov; Anita.Garg-1@nasa.gov; Darrell.J.Gaydosh@nasa.gov

1359-6462/$ - see front matter Published by Elsevier Ltd. on behalf of Acta Materialia Inc.
doi:10.1016/j.scriptamat.2010.12.028

loading of the same sample while preventing buckling in compression. Finally, the machined samples were double wrapped in Ta foil, heat treated under flowing argon for 3 h at 550 °C to form a two-phase structure and air cooled. All samples were characterized microstructurally and mechanically in this heat-treated state.

The $Ni_{50.3}Ti_{29.7}Hf_{20}$ samples were characterized mechanically via load-biased thermal cycling and isothermal load/unload type superelastic testing at temperatures above A_F. Load-biased testing consisted of thermal cycles between 30 and 300 °C at constant engineering stress levels from 0 to 500 MPa in increments of 100 MPa on separate samples under tension and compression. At each stress level, the sample was loaded to the desired stress at 30 °C in the martensite state and then underwent two heat–cool thermal cycles. The stress was then incremented to the next load level and the process repeated. Data from the second thermal cycle at each stress level was used to measure unrecovered strain (a measure of dimensional stability), transformation temperatures and transformation strain. The latter property was used to calculate work output according to the equation work = applied engineering stress × transformation strain. Separate superelastic tests were also conducted under tension at 180, 200 and 220 °C by heating to the test temperature, allowing the temperature to stabilize for approximately 5 min, loading under a controlled strain rate of 1×10^{-4} s^{-1} to 3% engineering strain, then unloading at the same strain rate to zero load. Apparent moduli at each temperature were measured from the engineering stress–engineering strain data, along with other properties, including 0.2% offset yield stress, slopes of the loading and unloading plateaus, and mechanical hysteresis. Additional details of the mechanical test procedures can be found in Ref. [11].

Microstructural analysis of the heat-treated material was conducted via transmission electron microscopy (TEM) using a FEI CM200 microscope, which revealed a B19′ monoclinic matrix and a fine twin variant martensite structure at room temperature (Fig. 1). At higher magnification, a homogeneous dispersion of fine precipitates was clearly visible, with precipitate sizes on the scale of 10–20 nm. Preliminary diffraction analysis indicated that this fine precipitate phase has a complicated structure and is neither a $Ni_4(Ti, Hf)_3$-type phase, as reported by Meng et al. in a $Ti_{29.2}Ni_{50.8}Hf_{20}$ alloy [3], nor the P-phase observed by Kovarik et al. [8] in a slightly Ni(Pt)-rich NiTiPt alloy. Detailed analysis of the crystal structure of this phase is currently underway.

The results of load-biased thermal cycles under tension and compression are shown in Figure 2. Straight-line segments were fitted to the resulting true strain–temperature data using linear regression in each of three sections: the martensite coefficient of thermal expansion (CTE) region, the transformation region (fitting to the region of maximum slope) and the austenite CTE region. Transformation temperatures during heating (A_S, A_F) and cooling (M_S, M_F) were calculated using the intersections of the fit lines from stress-free and load-biased thermal cycles and are summarized in Table 1. No-load transformation temperatures show an average improvement from heat treatment of 49 °C over the as-extruded M_F, M_S, A_S and A_F of 71, 87, 109 and 123 °C, respectively.

The $Ni_{50.3}Ti_{29.7}Hf_{20}$ alloy exhibits a strong asymmetry under tensile vs. compressive load-biased thermal cycling. This is evident in the factor of ~2 difference in stress dependence of the transformation temperatures and in the transformation strain/work output (Fig. 2). Under load-biased thermal cycling, the A_S and M_F temperatures show a linear stress dependence of approximately 7–8 °C/100 MPa under tension and 3–4 °C/100 MPa in compression over the entire stress range. The A_F and M_S temperatures exhibited a bilinear behavior with a dependence of 6 and 8 °C/100 MPa, respectively, under tension and 3 and 5 °C/100 MPa, respectively, in compression from 0 to 200 MPa. From 200 to 500 MPa, there is an increased effect of stress on transformation temperatures, with A_F and M_S rising to 13 and 14 °C/100 MPa, respectively, under tension and to 7 °C/100 MPa for both temperatures in compression. Thermal hysteresis, measured as A_F–M_S, decreases with increasing stress from 29 to 22 °C under tension and from 28 to 25 °C in compression (Table 1).

Transformation strain during load-biased thermal cycling increased with increasing stress from 1.68% at 100 MPa to 3.74% at 500 MPa under tension and from −0.71% at −100 MPa to −2.24% at −500 MPa in compression (Table 2). It is clear from the rate of increase in the transformation strain with stress that the peak transformation strain was not reached even at 500 MPa under tension or compression. This suggests that it could still be possible to produce higher transformation strains if higher stresses were applied. It also indicates that the

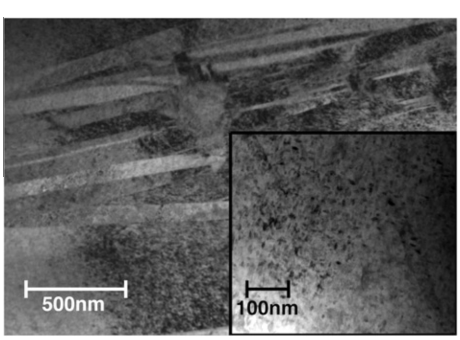

Figure 1. Bright-field TEM micrograph showing the microstructure of the aged $Ni_{50.3}Ti_{29.7}Hf_{20}$ alloy at room temperature, consisting of twin variants and high-density homogeneously distributed nanometer-size fine precipitates (inset).

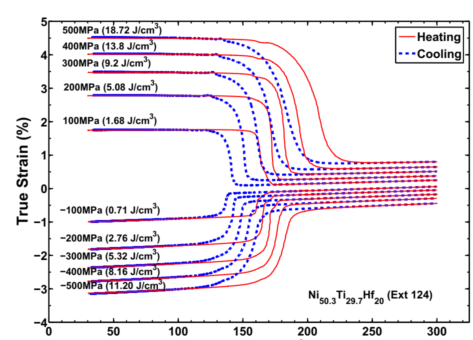

Figure 2. Load-biased shape memory behavior of aged $Ni_{50.5}Ti_{29.7}Hf_{20}$ under tension and compression. Note the tension–compression asymmetry and the closed strain–temperature loops demonstrating excellent dimensional stability.